

Supplementary information

A microfluidic platform for generating large-scale nearly identical human microphysiological vascularized tissue arrays

Yu-Hsiang Hsu^{a†}, Monica L. Moya^{a†}, Christopher C.W. Hughes^{ab}, Steven C. George^{acd¶}, Abraham P. Lee^{ac¶*}

^a Department of Biomedical Engineering, ^b Molecular Biology and Biochemistry, ^c Chemical Engineering and Materials Science, ^d Medicine, ^e Mechanical and Aerospace Engineering, University of California, Irvine, CA 92697 USA

* Tel: +1-(949) 824-9691; Fax: +1-(949) 824-1727; E-mail: aplee@uci.edu, 3120 Natural Sciences II, Irvine, CA 92697-2715, USA

Design of a microtissue array with a spectrum of different microphysiological environment

Figure S1(A) shows an example of an equivalent circuit that could provide a different pressure drop across n microtissue chambers. The constant pressure drop (ΔP_L) across each two-terminal component (R_{Li}) is controlled by designing the length of the microchannel segment connected in parallel with each microtissue chamber. This is equivalent to control the hydraulic resistance of the numerator of the pressure divider. The constant pressure drop ΔP_{Li} for the i -th component can be written as,

$$\Delta P_{Li} = \frac{\sum_{k=i}^{n+1} R_k}{\sum_{j=1}^{n+1} R_j} \Delta P = \frac{\sum_{k=i}^{n+1} R_k}{R_T} \Delta P. \quad (S1)$$

Considering the case that the length of each segment ($R_2 = R_3 = \dots = R_{2n} = R$) is identical, Eq. (S1) can be further simplified to

$$\Delta P_{Li} = \frac{(2i-1)R}{R_T} \Delta P. \quad (S2)$$

By using this approach, the magnitude of pressure drop across each microtissue chamber is increased with a fixed value $2R\Delta P/R_T$. Figure S1(B) shows the pressure field of a design of microfluidic platform based on Eq. (S2), where the basic configuration is the same with the one discussed in Fig. 3. The total length of the long microchannel is 575 mm, and the total pressure drop is also maintained at 10 mmH₂O (98.1 Pa). It clearly demonstrated that a relative low pressure drop can be applied to a microtissue chamber with a short segment of microchannel (the first on the right), and a high pressure drop can also be achieved to another one with a longer microchannel segment (increased from right chamber to the left one). This effect is also evidenced by the velocity field shown in Fig. S1(C), where the magnitude of velocity field of the microtissue chamber connected to a longer segment of microchannel has a higher magnitude of velocity profile. This effect is also verified by comparing the simulated pressure field and velocity field across each microchamber from the communication pore at high pressure to the low pressure side. Figure S1(D) shows the data lines of the pressure fields, where the corresponding pressure field is labelled from C1 to C12 to represent the microtissue chambers receiving high pressure drop to low pressure drop shown in Fig S1(B) and S1(C). Varied velocity profiles with different magnitudes are also verified and are shown in Fig. S1(E). It demonstrated that the magnitude of interstitial flow can be fine controlled in each microtissue chamber even each chamber is physically connected with a necking channel.

This example demonstrates that the present microfluidic configuration and method could potentially be generalized to systematically study cellular response to different microphysiological environment. It could also have a broader impact to understand microvascular formation, tissue development, tumour formation, and other tissue engineering applications.

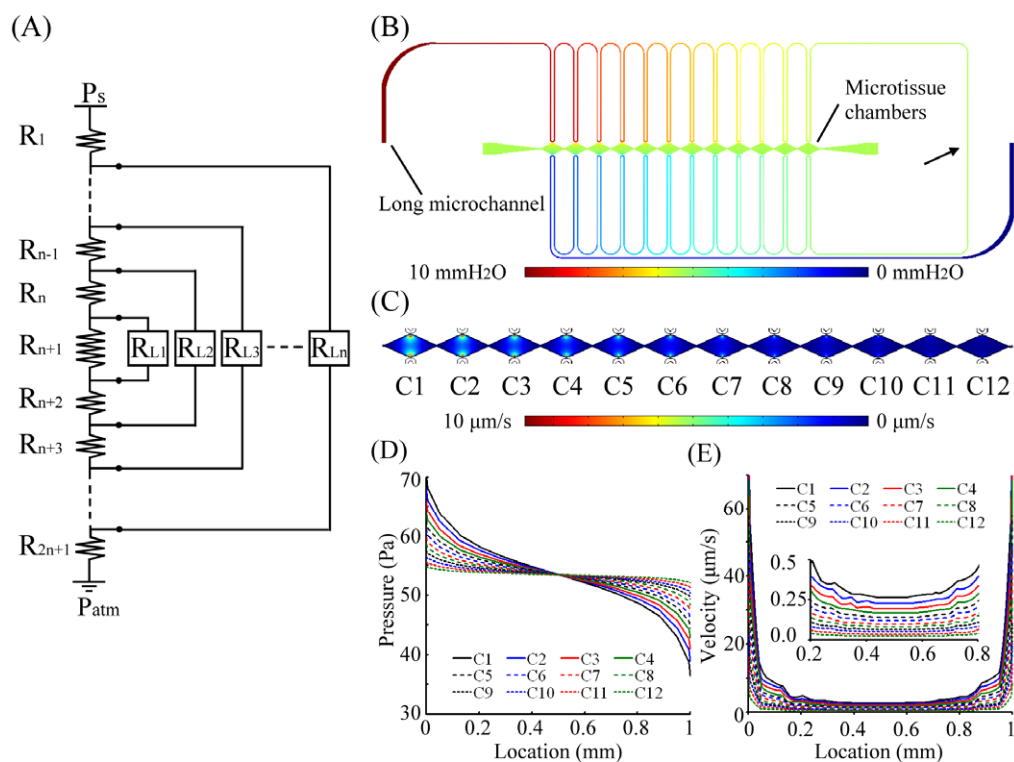


Fig. S1 (A) An Equivalent circuit of a long microchannel connected by n external loadings with different pressure drop, and (B) a microfluidic configuration and the simulated pressure field of the multi-microtissue platform with a spectrum of different physiological environment, (C) simulated velocity field of each microtissue chambers, (D) & (E) the pressure field and velocity field of each microtissue chamber.